Free-Carrier Generation in Aggregates of Single-Wall Carbon Nanotubes by Photoexcitation in the Ultraviolet Regime

Jared J. Crochet, Sajjad Hoseinkhani, Larry Lüer, Tobias Hertel, Stephen K. Doorn, and Guglielmo Lanzani

Phys. Rev. Lett. **107**, 257402 — Published 16 December 2011

DOI: 10.1103/PhysRevLett.107.257402

Free-carrier generation in aggregates of single-wall carbon nanotubes by photoexcitation in the ultraviolet regime

Jared J. Crochet,[1,*] Sajjad Hoseinkhani,[2] Larry Lüer,[3] Tobias Hertel,[4] Stephen K. Doorn,[1] and Guglielmo Lanzani[5]

[1] *Center for Integrated Nanotechnologies, Los Alamos National Laboratory, New Mexico, USA*[†]
[2] *CNR/INFM-ULTRAS, Politecnico di Milano, Milan, Italy*[‡]
[3] *Madrid Institute of Advanced Studies, IMDEA Nanociencia, Madrid, Spain*
[4] *Institute for Physical and Theoretical Chemistry & Department of Chemistry and Pharmacy, University of Würzburg, Würzburg, Germany*
[5] *Center for Nanoscience and Technology of IIT @ POLIMI and Physics Department of Politecnico di Milano, Milan, Italy*

We present evidence for the generation of free-carriers in aggregated single-wall carbon nanotubes by photoexcitation in the energetic range of the $\pi \rightarrow \pi^*$ transition associated with the M saddle point of the graphene lattice. The underlying broad absorption culminating at 4.3 eV can be fit well with a Fano line shape that describes strong coupling of a saddle point exciton to an underlying free electron hole pair continuum. Moreover, it is demonstrated that transitions in this energetic region autoionize into the continuum by detecting features unique to the presence of free charges in the transient transmission spectra of the continuum embedded second sub-band exciton, S_2.

PACS numbers: 61.48.De, 78.67.De, 78.67.Sc
Keywords: carbon nanotube, charge transfer, Stark effect, saddle point, exciton, bundle

Single-wall carbon nanotubes (SWNT) can be thought of as circumferentially quantized graphene tubules whose electronic properties depend strongly on chirality[1]. The primary photoexcitations of un-aggregated semiconducting tubes consist of several manifolds of highly anisotropic, strongly bound excitons[2]. It is known however that in semiconducting SWNTs the free-carrier response increases as a function of aggregate size[3]. From a phenomenological perspective, this observation can be interpreted as screening of the quasi-1D Coulomb interaction that leads to an enhanced response of the free-carrier continuum[4]. In SWNTs, this increase in the continuum optical response culminates at an ≈ 4.5 eV $\pi \rightarrow \pi^*$ transition arising from the graphene M saddle point[5]. Interestingly, the M point transition in graphene is largely affected by excitonic effects[6] and gives rise to a Fano line shape absorbance that strongly alters the universal optical conductance of $\pi e^2/2h$ above the infrared spectral range[7, 8]. It is understood that this exciton is extremely short lived (< 1 fs), undergoing autoionization into the underlying free-carrier continuum. Nevertheless, the nature and role that the M point transition as well as free-carriers have in the photophysics of SWNTs in isolated and aggregated form is of fundamental and applied interest[9, 10].

Here we present a series of excitation energy dependent transient transmission ($\Delta T/T_0$) experiments on predominantly aggregated (6,5) SWNTs (CoMoCAT SG-65) embedded in a thin film gelatin matrix[11, 12]. We find $\Delta T/T_0$ under UV excitation near the M point, where the electronic density of states is the largest[13], differs strongly from resonant S_1 or S_2 excitation. A Fano line shape absorption of the M point transition as well as a dynamic Stark shift coupled with a strong photoinduced absorption of the continuum embedded S_2 exciton, provide strong evidence for the photo-generation of free charges *via* autoionization upon UV excitation. This investigation experimentally illustrates how electronic dimensionality can be altered in a SWNT aggregate by nearest neighbor interactions through charge transfer excitons[14], and emphasizes the prospect of SWNT networks for light harvesting applications.

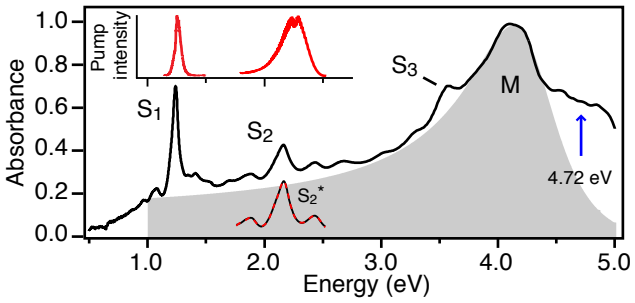

FIG. 1. Absorption spectrum of SWNT sample. The exciton resonances S_i are labeled and the grey shaded region is a Fano fit to the M point exciton. The red dashed line indicated by S_2^* is a multi-peak fit to the excitonic part of the S_2 region. The inset shows the excitation pulse spectra and the blue arrow indicates third harmonic excitation.

A standard pump-probe configuration was used to measure differential transient transmission $\Delta T/T_0$. The experimental set-up includes an amplified Ti:Sapphire laser (200μJ-1 kHz: 150fs) that drives two nonlinear optical parametric amplifiers (NOPAs). A white light continuum was generated by focusing a fraction of the fundamental beam on a thin sapphire plate. The continuum

* jcrochet@lanl.gov
† current address: Physical Chemistry and Applied Spectroscopy, Los Alamos National Laboratory, New Mexico, USA
‡ current address: Department of Material Science, University of Milano-Bicocca, Milan, Italy

was amplified in a barium borate crystal by pumping with the second harmonic at 390 nm. Broadband pulses were generated in visible, 1.8-2.4 eV, and infrared, 0.82-1.4 eV, spectral ranges and compressed on a set of doubly chirped mirrors to pulse widths of ≈ 10 and 15 fs respectively. Excitation at 4.72 eV was provided by the third harmonic of the Ti:sapphire fundamental with a pulse width of ≈180 fs. The probe light consisted of the NOPA output or the white light continuum. Data acquisition was carried out via a computer controlled optical multichannel analyzer that allowed for recording $\Delta T/T_0$ as a function of time delay between pump and probe pulses and as a function of probe wavelength.

Fig. 1 shows the ground state absorption spectrum of a SWNT-gelatin film. The exciton resonances S_1-S_3 can be observed at 1.25, 2.16[15], and 3.6 eV[16] residing on a broad background culminating at the $\pi \rightarrow \pi^*$ transition at approximately 4.3 eV. Motivated by recent investigations of the M point exciton in graphene we fit this feature with a Fano profile $A(E) \propto (q+\epsilon)^2/(1+\epsilon^2)$ where $\epsilon = (E - E_r)/(\Gamma/2)$. Here q^2 defines the ratio of the strength of the excitonic transition to the free $\pi \rightarrow \pi^*$ transition, E_r is the exciton resonance energy, and Γ corresponds to the exciton lifetime[7]. We find within this model that E_r =4.28 eV, Γ =860 meV (≈ 5 fs), and q =-2.83 fits the shape of the underlying absorbance sufficiently up to approximately 1 eV. This is similar to graphene where at approximately 1 eV the Fano tail no longer fits the optical conductivity[7]. Also, at higher energies than 4.5 eV the absorbance is not very well resolved because of strong absorption by the gelatin matrix. It is important to note that the E_r for this chirality range of SWNTs is approximately 700 meV smaller than what is measured in both single and few layer graphene, indicating, as predicted, strong modifications in the $\pi \rightarrow \pi^*$ transition occur upon rolling the graphene sheet[5].

In Figs. 2a-2c, time-resolved $\Delta T/T_0$ spectra in the vicinity of the S_2 exciton are shown in a color-coded representation. Here strong photoinduced or excited state absorption (PA, $\Delta T/T_0 < 0$) is shaded blue and strong photobleach or ground state bleaching (PB, $\Delta T/T_0 > 0$) is shaded red. Resonantly exciting the low energy excitons (S_1-1.4×10^{15} cm^{-2}, S_2-2.5×10^{15} cm^{-2} in Fig. 2a and 2b, respectively) the apparent magnitude of the PA is smaller than the PB. In the specific case of resonantly exciting S_2, Fig. 2b, we observed initially a broad PB which narrows down to the same width of Fig. 2a within approximately 50 fs. The initial broadening is caused by broadband excitation of energetically neighboring S_2 excitons (belonging to other impurity (n,m) species) in contrast to Fig. 2a where the excitation energy is resonant predominantly with the (6,5) tube. Hence, broadband excitation results in the resonant excitation of minority tube species through S_2 including the (6,4) and (8,3) tubes which initially contribute to the $\Delta T/T_0$ spectra. Recently, we have shown that the spectral narrowing observed here is caused by a two step process that involves an S_2 to S_1 internal conversion in ≈ 40 fs followed by resonance energy transfer from the minority tubes towards the majority (6,5) tube or towards other smaller band gap tubes within 10 fs[17]. We have also shown that the apparently delayed formation of the PA (Fig. 2b) occurs only in aggregates, while in isolated tubes, the PA forms during the excitation pulse.

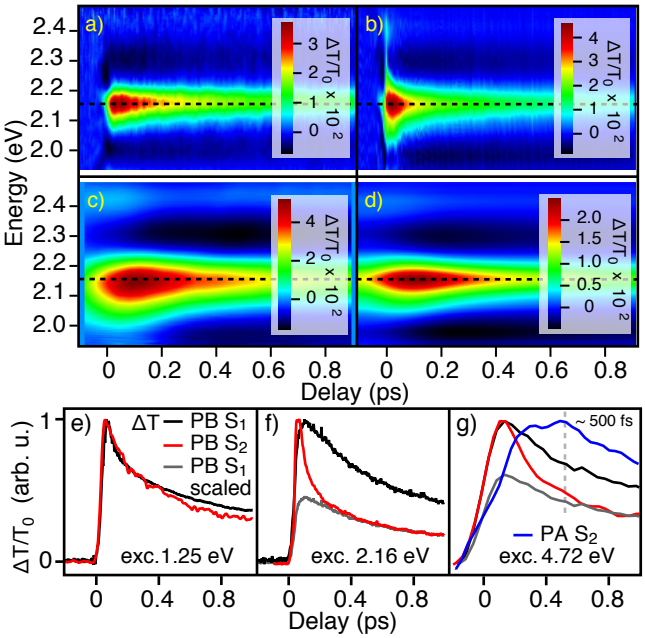

FIG. 2. $\Delta T/T_0$ spectra around the S_2 (dashed line) after excitation at 1.25, 2.17, and 4.72 eV (panels a, b, and c respectively). The time resolution is approximately 10, 20, and 100 fs for panels a, b, and c. Panel d shows a replica of panel e that has been convoluted by a 100 fs Gaussian along the time direction. Normalized $\Delta T/T_0$ traces in the maxima of the PB bands of S_1 and S_2 (red and black curves, respectively) exciting at 1.25, 2.15, and 4.72 eV are shown in panels e, f, and g. Grey traces in panels f and g are replicas of the black traces scaled to match the red curves after initial relaxation and the blue trace in g is the maxima of the PA band in c.

In contrast, exciting at 4.72 eV (8.3×10^{14} cm^{-2}), the PA and the PB have similar spectral weight at early delay times, and for longer times the PA becomes dominant in the $\Delta T/T_0$ spectra centered at ≈ 2.3 eV, Fig. 2c. Moreover, the maximum PA occurs after ≈ 500 fs compared to ≈ 200 fs after resonantly exciting S_2 and less than 10 fs after resonantly exciting S_1. In order to further emphasize the difference between exciting at 4.72 eV and S_2, we show in Fig. 2d how the dynamics of resonant S_2 excitation appear after convolution with a 100 fs Gaussian pulse. As expected, the initial broadening is not resolved; however, clear differences between Fig. 2c and Fig. 2d remain. In Fig. 2d the maximum PA is reached within 200 fs and is stronger on the red side than on the blue side as in Fig. 2b. We can therefore conclude that UV excitation introduces an additional process which is superimposed on intertube energy-transfer effects observed at low energy excitation.

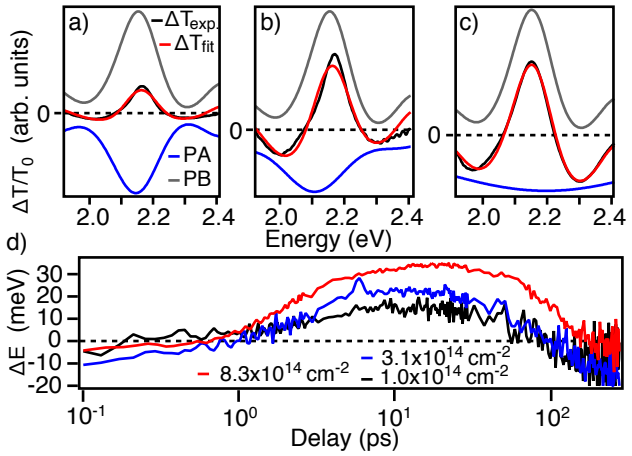

FIG. 3. Decomposition of $\Delta T/T_0$ spectra at t = 900 fs for S_1, S_2 and 4.72 eV excitation (a, b, and c respectively). The PB contribution (grey curve) is a vertically scaled replica of the excitonic part of the ground state absorption, while the PA contribution (blue curve) is calculated as an inverted, vertically scaled, shifted and broadened replica of the PB contribution. d) Fluence dependence of the dynamical shift of the S_2 PB exciting at 4.72 eV.

Further insight is gained from analyzing the maximum PBs of S_1 and S_2 for different excitation conditions. As shown in Fig. 2e, we find upon resonant excitation of S_1 both PBs of S_1 and S_2 form together and decay similarly during the first 400 fs. However, resonantly exciting S_2, Fig. 2f, we find a delayed rise of the PB of S_1 with a simultaneous decay of the PB of S_2 which was previously assigned to an ultrafast internal conversion of S_2 to S_1[18]. Subsequently, the PBs S_1 and S_2 decay together starting within approximately 200 fs as shown by the scaled PB of S_1 (grey trace) in Fig. 2f. For 4.72 eV excitation, Fig. 2g, similar to resonant S_2 excitation we found a faster PB recovery of S_2 than of S_1. This is similar to what is observed while resonantly exciting S_2, but a closer look at the dynamics highlights an important difference. In Fig. 2g, the time resolution is not as good as in Fig. 2f because of the the longer excitation pulses at 4.72 eV, but it can be quite clearly observed that the time it takes for the two traces to reach a common decay is on the order of 500 fs, or approximately 2.5 times as much as in Fig. 2f, grey trace Fig. 2g. This observation can be attributed to a delayed relaxation process that occurs predominantly in the S_2 spectral region only after exciting at higher energies and coincides with the maximum PA signal, Fig. 2g.

We performed a multi-Gaussian analysis of vertical cuts of Figs. 2a-c at t = 900 fs (subsequent to energy transfer and internal conversion dynamics), Figs. 3a-c. In the analysis, we simulated the PB by a scaled replica of the excitonic part of the ground state absorption spectrum which represents ground state bleaching while simulating the PA as an inversely scaled, broadened, and energetically shifted replica of the PB to represent excited state absorption. Reasonable agreement was found for all the three excitation conditions. For low-energy excitation, red-shifts of the PA less than 50 meV and small broadening values less than 100 meV were obtained, while for UV excitation a blue-shift was observed of $\approx$ 60 meV and the broadening was very strong, in excess of 500 meV. The analysis suggests that there is a single PA band in the $\Delta T/T_0$ spectra, which is broader than PB and becomes dominant in the edges of the transient transmission spectrum yielding $\Delta T/T_0$ <0. As in quantum wells, this broadening of the excited state can be attributed to scattering of the exciton with the continuum in which it is embedded[19, 20]. Supporting this conjecture, we found the spectral position of the S_2 PB maximum for UV excitation, as opposed to low energy excitation, was strongly time dependent. As shown in Fig. 3d, the PB was dynamically shifted with respect to the S_2 ground state absorption energy and depended strongly on fluence. The S_2 PB was initially red-shifted by 10s of meV and within 20 ps was blue-shifted to a maximum of 10s of meV followed by a slow recovery back to the ground state energy. In light of these three findings, which include a delayed relaxation pathway coinciding with an extremely broad strong PA and a fluence dependent dynamic spectral shift of the S_2 PB, we discuss how photo-generated free-carriers near the M point can alter the $\Delta T/T_0$ spectra near S_2 through charge transfer states.

First, we ruled out the possibility of thermal or mechanical effects that could lead to our observations. If upon the absorption of UV photons the SWNT film underwent an increase in temperature a spectral shift would be observed, however, as shown by Li *et al* and Karaiska *et al* heating the (6,5) tube would result in a redshift of the transition energy which is mostly due to strain[21, 22]. Moreover, in the absence of strain it is predicted that the band gap of the (6,5) tube will be reduced upon a temperature increase[23]. Nonetheless, recent continuous wave PA experiments have provided strong evidence for long-lived trapped charges in similar samples under visible photo-excitation[24].

Electric field effects in 1D excitonic systems have been predicted to include strong field strength dependent broadenings and spectral shifts[25]. Within the quadratic Stark effect description, the shift (ΔE_x) of the ground state exciton energy (E_x) can be expressed as $\Delta E_x = \sum_j |\vec{\mu_j} \cdot \vec{F}|^2/(E_x - E_j)$ where $\vec{F}$ is the electric field strength and $\vec{\mu_j}$ and E_j are the dipole moment and energy of continuum state j. The denominator of ΔE_x determines the sign of the shift, where coupling to higher or lower energy continuum states results in a red- or blue-shift, respectively. Here, auto-ionization of M point excitons initially lead to a finite population of high energy continuum states that red-shift S_2. The build up of a strong PA within 500 fs coincides with a sign change in ΔE_x, therefore lower energy continuum states within the energetic range S_2 are populated after interband relaxation, Fig. 4a. Thus, we assign the PA to a broadening

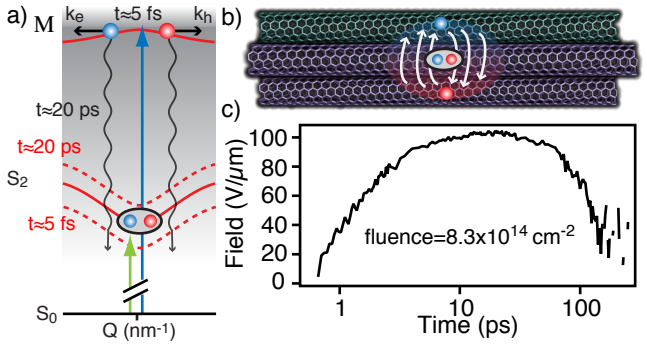

FIG. 4. a) Schematic of the electronic structure of a semiconducting SWNT with S_2 and the M point exciton. The unperturbed S_2 exciton energy is given by the solid band. Early, ≈5 fs, dynamics upon UV photoexctitation lead to a red Stark shift of the S_2 exciton. Later dynamics, ≈20 ps, are where higher lying electron-hole pairs fully relax to energies below the S_2 exciton leading to a blue Stark shift. b) Schematic of an internal field in a SWNT aggregate because of free charges in close proximity to an exciton. c) Estimated field strength from the dynamic blue-shift of S_2 described in the text.

or enhanced dephasing of S_2 induced by hot free-carriers. The slow recovery of ΔE_x to the S_2 ground state energy reflects electron-hole pair recombination which occurs on a time scale of 100s of ps. Moreover, the strong fluence dependence of the shift of the maximum PB in Fig. 3d is understood from the strong field dependence of ΔE_x, in which F is proportional to the local charge density excited by the pump pulse and stabilized within an aggregate, Fig. 4b. The magnitude of F can be estimated from the Stark shift of one-dimensional Wannier excitons, $\Delta E_x \approx 9e^2 r_0^2 F^2/8E_b$[26], where $E_b = 350$ meV is the exciton binding energy and $r_0 = 1.0$ nm is the exciton radius, Fig. 4c. From the maximum blue-shift of S_2 in Fig. 3d we estimated field strengths of up to $F \approx 100$ V/μm , which is consistent with previous measured SWNT Stark shifts by the displacement photocurrent technique[27].

Concluding, we emphasize the importance of free-carrier transitions beyond an excitonic picture in describing the optical response of SWNT aggregates. Strong absorption strengths in the UV combined with exciton dissociation highlight an opportunity to further investigate related photovoltaic effects. Additionally, unusually large Franz-Keldysh oscillations at UV wavelengths in SWNTs have been previously observed by Ham *et al*[28], and our findings provide a mechanism for generating the un-bound electron-hole pairs that underline this behavior. In light of our findings, we expect that density gradient ultracentrifugation will be used as a tool to sort well defined SWNT samples as a function of aggregate size to uncover systematic variations in excitonic and free carrier responses[3]. Finally, we make the connection between a microscopic scattering mechanism and changes in the macroscopic dielectric function which alter the dimensionality of nearly ideal 1D semiconductors through an enhanced response of the underlying charge transfer continuum.

ACKNOWLEDGMENTS

This work was financially supported by the European Commission through the Human Potential Programme (Marie-Curie RTN BIMORE, Grant No MRTN-CT-2006-035859), and performed, in part, at the Center for Integrated Nanotechnologies, a U.S. Department of Energy, Office of Basic Energy Sciences user facility.

[1] S. Reich, C. Thomsen, and J. Maultzsch, *Carbon Nanotubes: Basic Concepts and Physical Properties* (Wiley - VCH, 2004).
[2] K. Sato, R. Saito, J. Jiang, G. Dresselhaus, and M. S. Dresselhaus, Phys. Rev. B **76**, 195446 (2007).
[3] J. J. Crochet, J. D. Sau, J. G. Duque, S. K. Doorn, and M. L. Cohen, ACS Nano **5**, 2611 (2011).
[4] T. Ogawa and T. Takagahara, Phys. Rev. B **44**, 8138 (1991).
[5] Y. Takagi and S. Okada, Phys. Rev. B **79**, 233406 (2009).
[6] L. Yang, J. Deslippe, C.-H. Park, M. L. Cohen, and S. G. Louie, Phys. Rev. Lett. **103**, 186802 (2009).
[7] K. F. Mak, J. Shan, and T. F. Heinz, Phys. Rev. Lett. **106**, 046401 (2011).
[8] D.-H. Chae, T. Utikal, S. Weisenburger, H. Giessen, K. v. Klitzing, M. Lippitz, and J. Smet, Nano Lett. **11**, 1379 (2011).
[9] Y. Murakami and S. Maruyama, Phys. Rev. B **79**, 155445 (2009).
[10] M. C. Beard, J. L. Blackburn, and M. J. Heben, Nano Letters **8**, 4238 (2008).
[11] J. Crochet, M. Clemens, and T. Hertel, J. Am. Chem. Soc. **129**, 8058 (2007).
[12] J. Crochet, M. Clemens, and T. Hertel, Phys. Status Solidi B **244**, 3964 (2007).
[13] K. De Blauwe, D. J. Mowbray, Y. Miyata, P. Ayala, H. Shiozawa, A. Rubio, P. Hoffmann, H. Kataura, and T. Pichler, Phys. Rev. B **82**, 125444 (2010).
[14] G. D. Scholes, ACS Nano **2**, 523 (2008).
[15] S. M. Bachilo, M. S. Strano, C. Kittrell, R. H. Hauge, R. E. Smalley, and R. B. Weisman, Science **298**, 2361 (2002).
[16] E. H. Haroz, S. M. Bachilo, R. B. Weisman, and S. K. Doorn, Phys. Rev. B **77** (2008).
[17] L. Lüer, J. Crochet, T. Hertel, G. Cerullo, and G. Lanzani, ACS Nano **4**, 4265 (2010).
[18] C. Manzoni, A. Gambetta, E. Menna, M. Meneghetti, G. Lanzani, and G. Cerullo, Phys. Rev. Lett. **94**, 207401 (2005).
[19] S. Schmitt-Rink, D. S. Chemla, and D. A. B. Miller, Phys. Rev. B **32**, 6601 (1985).
[20] L. Schultheis, J. Kuhl, A. Honold, and C. W. Tu, Phys.

Rev. Lett. **57**, 1635 (1986).
[21] L.-J. Li, R. J. Nicholas, R. S. Deacon, and P. A. Shields, Phys. Rev. Lett. **93**, 156104 (2004).
[22] D. Karaiskaj, C. Engtrakul, T. McDonald, M. J. Heben, and A. Mascarenhas, Phys. Rev. Lett. **96**, 106805 (2006).
[23] R. B. Capaz, C. D. Spataru, P. Tangney, M. L. Cohen, and S. G. Louie, Phys. Rev. Lett. **94**, 036801 (2005).
[24] C. Sciascia, J. Crochet, T. Hertel, and G. Lanzani, Eur. Phys. J. B **75**, 115 (2010).
[25] V. Perebeinos and P. Avouris, Nano Lett. **7**, 609 (2007).
[26] G. Weiser, Phys. Rev. B **45**, 14076 (1992).
[27] A. D. Mohite, P. Gopinath, H. M. Shah, and B. W. Alphenaar, Nano Lett. **8**, 142 (2007).
[28] M.-H. Ham, B.-S. Kong, W.-J. Kim, H.-T. Jung, and M. S. Strano, Phys. Rev. Lett. **102**, 047402 (2009).